Surface Segregation During Irradiation

L.E. Rehn and N.Q. Lam

Abstract. Gibbsian adsorption is known to alter the surface composition of many alloys. During irradiation, four additional processes that affect the near-surface alloy composition become operative: preferential sputtering, displacement mixing, radiation enhanced diffusion, and radiation induced segregation. Because of the mutual competition of these five processes, near-surface compositional changes in an irradiation environment can be extremely complex. Although ion-beam induced surface compositional changes were noted as long as 50 years ago, it is only during the past several years that individual mechanisms have been clearly identified. In this paper, a simple physical description of each of the processes is given, and selected examples of recent important progress are discussed. With the notable exception of preferential sputtering, it is shown that a reasonable qualitative understanding of the relative contributions from the individual processes under various irradiation conditions has been attained. However, considerably more effort will be required before a quantitative, predictive capability can be achieved.

INTRODUCTION

Compositional changes which occur in the surface and near-surface regions of an alloy during irradiation with energetic particles are important in many areas of materials science. For example, ion bombardment is used routinely to prepare clean surfaces, and in conjunction with several surface-sensitive techniques, to depth-profile the composition of an alloy beneath an exposed surface. Plasma contamination from sputtered atoms is a serious concern in the operation of existing fusion devices, and its importance will grow as energy output levels increase. Techniques such as sputter deposition, ion implantation and ion-beam mixing are currently being used to modify surfaces of materials for a wide variety of technological applications. A fundamental understanding of how irradiation alters near-surface alloy compositions therefore provides a foundation for future advances in many different areas.

The thermodynamic basis for equilibrium surface segregation was formulated by Gibbs in the previous century. Wynblatt et al. [1] have reviewed recent progress in understanding equilibrium (Gibbsian) segregation. Several additional, nonthermodynamic driving forces for surface segregation manifest themselves during irradiation with energetic particles (electrons, gamma rays, ions, or neutrons) [2–5]. Because large numbers of excess point defects are created, one effect of irradiation is simply to enhance the rate at which Gibbsian surface segregation approaches equilibrium. In addition to this radiation enhanced diffusion, there exist at least three other kinetic effects which can alter the near-surface composition of an alloy during irradiation: displacement mixing, preferential sputtering, and radiation induced segregation. For the sake of completeness, two additional processes that produce compositional changes during irradiation should be mentioned, ion implantation and nuclear transmutations. However these latter effects are highly specific to the type of irradiation particle, and therefore will not be covered in this review. For the purposes of this symposium, we focus on those compositional changes which occur at or very close to the irradiated surface. A recent review which emphasizes effects at greater depths can be found elsewhere [6].

During irradiation, incoming particles displace lattice atoms off their normal sites into interstitial positions. In metals, the kinetic energy from these localized displacement events is dissipated in extremely short times ($\leq 10^{-11}$ s). Sputtering of atoms from the surface and displacement mixing of lattice atoms occur during

this brief period. In contrast, radiation enhanced diffusion and radiation induced segregation require thermally activated migration of the vacancy and interstitial defects, and thus operate on a significantly longer time scale which, depending upon the specimen temperature, can vary from fractions of a second up to very long periods. The net compositional changes which occur reflect the mutual competition of all five processes integrated over the experimental time interval.

From a theoretical standpoint, this complex interplay among several different processes allows at present only qualitative estimates to be made of surface compositional changes during irradiation. The experimental situation is complicated primarily by two factors. First, since both binding energies and the distribution of displacement energy during irradiation depend upon some of the same physical parameters, for instance the relative atomic masses and sizes of the alloying components, it is usually not possible to adjust the experimental conditions in a manner which ensures that only one process is significantly affected. Second, practically all experimental techniques average compositions over the depth from the surface in a manner which is understood only semi-quantitatively at best. This latter shortcoming in particular has lead to considerable controversy in comparing results obtained by different techniques. Despite these difficulties, significant progress has occurred over the past five years, particularly in identifying the relative contributions from the different effects under various irradiation conditions. Unfortunately, as will be seen below, the one exception to this statement remains preferential sputtering. Although it was the earliest anticipated effect, and although very strong arguments can be made for its existence, no clear demonstration of preferential sputtering in an alloy has yet been reported.

A simple physical description of each of the four kinetic processes which produce surface and near-surface compositional changes during irradiation is presented in the following sections, along with selected examples of recent progress in understanding individual contributions under various irradiation conditions. Following the natural time development, we begin by discussing the two effects which occur during the brief defect production event, preferential sputtering and displacement mixing, then turn our attention to the two defect migration assisted processes, radiation enhanced diffusion and radiation induced segregation.

PREFERENTIAL SPUTTERING

Collisions of lattice atoms with incoming particles cause target atoms to be ejected through the surface layer. Because surface binding energies are relatively small compared to displacement energies, many of the ejected

atoms are permanently removed from the specimen, that is, they are sputtered. The average range of the displaced atoms in a solid material is small, only two or three lattice distances. Hence sputtered atoms come predominantly from the top few atom layers.

Conservation of matter requires that after long times, the composition of the flux of atoms sputtered from an alloy must become equal to that of the bulk. Initially, however, the compositions of the sputtered atom flux and bulk are in general different, which produces a layer of altered composition in the near-surface region. Such changes are referred to generically as "preferential sputtering" effects. A recent extensive review of such effects has been given by Betz and Wehner [7].

There are strong reasons for expecting preferential sputtering to occur in most alloy systems under a wide variety of bombardment conditions. These reasons can be conveniently divided into two categories, mass and surface binding effects. Mass effects arise because the energy deposited in displacement events is generally not distributed equally among atoms of different masses, and also because lower mass atoms have larger projected ranges in a given material. Hence the probabilities for atoms of different masses in a given atomic layer of actually reaching the surface as a result of a displacement event are different. Differences in surface binding energies will cause preferential sputtering because the various components then require different amounts of energy to escape permanently through the surface. Two important similarities therefore exist between Gibbsian surface segregation and preferential sputtering. First, both sputtering and Gibbsian segregation affect predominantly the outermost atom layer. Second, those atoms which tend to Gibbsian-adsorb on the surface of a specimen, that is, those with the lower binding energies, are the same atoms which are expected to be preferentially sputtered from the surface.

It is important to realize that Gibbsian adsorption can cause a change in the near-surface composition of an alloy during sputtering even in the absence of all other effects. That is, any component which enriches in the surface layer will be preferentially removed simply because more of it is located in the layer from which most of the sputtered atoms are emitted. The similar consequences of preferential sputtering and Gibbsian segregation on the near-surface composition necessitate a stricter definition of preferential sputtering than initially provided above. Following Wiedersich [3], we write the yield, Y_i, of element i per incident ion as

$$Y_i = \sum_{x=1}^{\infty} P_{i,x} C_{i,x} \qquad (1)$$

where $P_{i,x}$ is the probability per incident particle that an i atom in atomic layer x is sputtered, and $C_{i,x}$ is the concentration of i atoms in layer x. The summation representation is chosen here to emphasize the discrete contributions from individual lattice planes to the sputtering process. In this form, the distinction first pointed out by Sigmund [8] between primary and secondary effects in alloy sputtering is made explicit. Primary effects are related to individual displacement events, and the pertinent physical parameters are contained in the $P_{i,x}$'s, that is, the type and energy of the incoming particles, the identity and surface binding energies of the target atoms, threshold displacement energies, projected ranges, etc. Secondary effects, which are discussed later in this paper, are those which alter the concentrations of individual atomic layers and thus enter Eq. (1) through $C_{i,x}$. Andersen [2] has offered a definition of preferential sputtering which incorporates only the primary effects. He states that preferential sputtering occurs if and only if the composition of the sputtered-atom flux differs from the appropriately-averaged composition of the atom layers contributing to that flux.

Under the previously often-employed assumption that atoms are sputtered from only the outermost atom layer, Eq. (1) may be used in conjunction with the steady-state conservation of matter restriction to write for a binary alloy composed of A and B atoms,

$$\frac{P_{A,l}C_{A,l}}{P_{B,l}C_{B,l}} = \frac{C_A^b}{C_B^b} \qquad (2)$$

where C_A^b and C_B^b are the bulk concentrations of A and B atoms, respectively. Hence, a measurement showing that the composition of the outermost layer at steady state was different from that of the bulk would provide a clear demonstration of preferential sputtering ($P_{Al} \neq P_{Bl}$) under the assumption that atoms are sputtered only from the top layer. Since ion surface scattering is essentially sensitive only to the composition of the outermost layer, such a demonstration is, in principle, quite straightforward.

Unfortunately, as discussed further under Defect Migration Processes, recent experimental as well as theoretical evidence indicates that a substantial fraction of sputtered particles, perhaps as much as 30 to 40%, are emitted from the second atomic layer. Under the assumption that two layers contribute to the sputtered flux, Eq. (2) becomes

$$\frac{P_{A,l}C_{A,l} + P_{A,2}C_{A,2}}{P_{B,l}C_{B,l} + P_{B,2}C_{B,2}} = \frac{C_A^b}{C_B^b}. \qquad (3)$$

Hence a demonstration of preferential sputtering assuming contributions from the top two atom layers requires measurements of the concentrations of these two layers, as well as of the fractional amount each layer contributes to the sputtered flux. Of course the inclusion of sputtered atoms from the third atomic layer would introduce two additional parameters to be measured. Measurements of this complexity have not yet been reported. Hence although ion-beam induced surface compositional changes were noted more than 50 years ago [7], and although our knowledge of surface binding energies and the distribution of kinetic energy among different-mass atoms in an alloy strongly supports its existence, true preferential sputtering of an alloy remains undemonstrated.

Although considered unlikely, we note that if the preferential sputtering contributions from different atom layers happened to be equal but opposite in sign, Andersen's definition in terms of the average composition would say that no preferential sputtering occurred. On a physical basis, therefore, a definition that preferential sputtering occurs whenever at least one $P_{ij} \neq P_{kj}$ appears more meaningful.

DISPLACEMENT MIXING

In addition to sputtering atoms from the surface, displacement events also force atoms to be exchanged between adjacent atomic planes, that is they rearrange or mix atoms within the target. Two different contributions to this mixing were recognized early, recoil implantation and cascade mixing. An ion beam enters the target with a net momentum directed toward the specimen interior. Since this inward momentum is not shared equally among different atomic species, some components will be driven, or recoil-implanted, deeper into the interior than other components. Sigmund and Gras-Marti [9] predicted that lighter elements will be recoil-implanted more efficiently than heavier elements, while computer simulation results by Roush et al. [10] have suggested the opposite behavior. Much of the energy of the incoming beam, however, is quickly distributed in a cascade of randomly directed displacements. Mixing due to these randomly directed displacement events is often referred to as cascade mixing.

Both recoil and cascade mixing have been observed in recent studies of marker layer motion during ion bombardment. In general, the magnitude of cascade mixing is found to be much larger than that due to recoil implantation [11]. Here we will use the term "displacement mixing" to describe all mass transport which occurs during the displacement event in the absence of any input of thermal energy from the surrounding lattice. That is, all atomic motion which occurs during the initial defect production stage, through the so-called "cooling phase" of the cascade, up to the time ($\sim 10^{-11}$ s in metals) when all the kinetic energy

from the displacement event has been dissipated into the surrounding material. This definition is quite useful from an experimental standpoint, since it ascribes to displacement mixing all atomic motion which is measured at temperatures low enough so that point defects remain immobile during an experiment.

Displacement mixing, even at temperatures low enough that thermally activated diffusion processes are completely negligible, will spread compositional changes induced in the outermost atom layers to greater depths. Such spreading is obviously confined to a layer roughly commensurate with the penetration range of the irradiation. Several atom replacements occur for each defect which is produced during irradiation; recent experiments in metals yield values of roughly 50 for the number of nearest-neighbor exchanges which occur per permanently displaced atom [11]. Hence energetic irradiation can produce very efficient mixing of target atoms.

Early evidence of the importance of displacement mixing during sputtering was obtained by Koshikawa et al. [12], who employed Auger electron spectroscopy (AES) to study near-surface compositional changes produced in Cu–Ni alloys by low-energy Ar bombardment at a specimen temperature of $-150°$ C. The low temperature was selected to eliminate any thermally activated, defect migration effects. Using Auger transitions of different energies, they found that the measured composition of the nickel-rich altered surface layer produced by the irradiation was, within experimental error, identical whether the signal was averaged over approximately the top 3–4 atom layers, or over a layer three to four times as thick. These results indicated that copper was being preferentially removed from the outermost layers, and that displacement mixing was spreading the nickel enrichment uniformly over depths at least as large as the projected ion range.

This simple picture of a uniformly mixed altered layer during sputtering changed shortly thereafter when Okutani et al. [13] reported their combined ion scattering spectroscopy (ISS) and AES study of similarly bombarded Cu–Ni targets. The new AES results again showed a uniformly mixed, nickel-rich surface layer, in agreement with the previous work. However the ISS measurements, which essentially monitor only the outermost atom layer, showed that in fact its composition was approximately equal to that of the bulk. If the commonly used assumption is made that sputtered atoms originate only from the top layer, the Okutani et al. results indicate that no preferential sputtering of copper has occurred, and therefore another mechanism must be responsible for the nickel-enriched layer. Their observation that displacement mixing did not generate a layer of uniform composition

in the near-surface region, but rather that a very steep concentration gradient was being created and preserved over the outermost few atom layers, is perhaps of even greater significance. Similar steep concentration gradients have also been observed by Andersen et al. [14], who used measured differences in the angular distribution of the sputtered components from a series of alloys to demonstrate that the outermost layer during ion bombardment is enriched, relative to the immediate subsurface layers, in that component which is known to Gibbsian-absorb. Again, a steep compositional gradient was found in the top few atom layers despite very low irradiation temperatures (77 K). At the low temperatures and high defect concentrations present in these experiments, thermally activated diffusion processes are negligible.

Since displacement mixing is the only mass transport mechanism operating at such low temperatures, the existence of the steep gradient and its strong correlation with surface binding energy demonstrate that displacement mixing is not simply a random collisional process, but rather that it can be influenced by thermodynamic forces. Over the past few years, several researchers in the ion-beam surface modification field have noted that ion-beam mixing of bilayer specimens also depends upon the thermodynamic properties of the materials that are mixed even at quite low irradiation temperatures. For example, Cheng et al. [15] found in several systems that the magnitude of mixing can be correlated with the heat of mixing calculated using Miedema's theory, as well as with the average heat of sublimation of the two bilayer materials. Work in this area has recently been reviewed by Averback [11]. A paper specifically addressing the role of thermodynamics in ion-induced atomic rearrangements in metals has been authored by Johnson et al. [16].

An example of these so-called chemical effects in ion-beam mixing, taken from the work of Averback et al., is given in Figure 1. Here Rutherford backscattering spectra taken before (solid line) and after (individual data points) ion beam mixing of two different bilayer specimens, Cu–Mo and Cu–Nb, are plotted. Mixing of the layers is indicated by a change in slope at both the leading edge of the copper signal, as well as at the trailing edge of the signal from the second element. Nb and Mo have nearly the same atomic masses, densities and melting points; there is virtually no mutual solid solubility of either with Cu. However, Cu–Mo has a much larger positive heat of mixing than does Cu–Nb. The difference in these thermodynamic variables is clearly manifested in the very low temperature (10 K) results, where mixing is significant in Cu–Nb, but much less occurs in Cu–Mo.
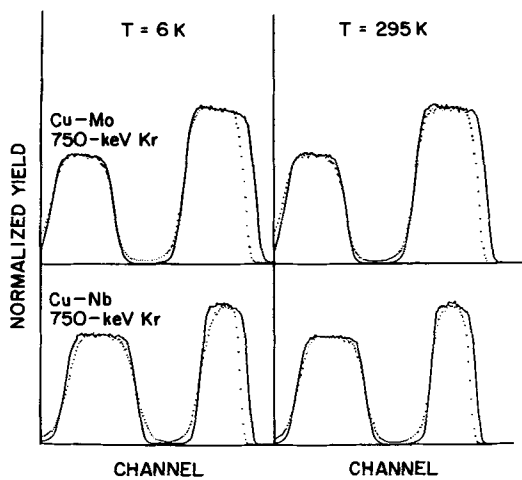
Fig. 1. Rutherford backscattering (RBS) spectra taken before (solid line) and after (individual data points) ion-beam mixing of Cu–Mo and Cu–Nb bilayer specimens with 750 keV Kr ions to a dose of 2×10^{16} cm^{-2} at 6 K and 295 K. The spectra have been shifted to account for the sputtering which occurred. Note that for Cu–Nb, which has a much larger positive heat of mixing, the mixing is significantly greater at 6 K than at 295 K.

We see from Figure 1 that the amount of mixing in Cu–Nb at room temperature is considerably reduced from the value obtained at 10 K. This is to be expected, since the additional defect mobility which occurs at the higher temperature should drive the target composition back toward equilibrium.

Such a temperature dependence, that is, where mixing at higher temperatures is less than at lower temperatures, may have important practical consequences for sputter-profiling of compositional gradients in metals. It is well known that the depth resolution of sputter-profiling techniques can degrade rapidly with increasing distance from the surface. This occurs primarily for two reasons [18], ion beam mixing of the compositional gradients and surface roughening. In order to minimize mixing, the general practice is to keep the specimen temperature as low as possible during sputtering to limit any contribution from radiation enhanced diffusion to mixing. Surface roughness effects, on the other hand, are known to decrease with increasing temperature [19]. Therefore it has long appeared that the temperature requirements for minimizing mixing and surface roughness effects on depth resolution were incompatible. Figure 1, however, shows that these two considerations are in fact compatible for materials with positive heats of mixing. In such cases, raising the specimen temperature can decrease both the amount of mixing and the surface roughness, thereby increasing the depth resolution.

Li, Koshikawa and Gato [20] have published a study

which offers further insight into the role of thermodynamic variables in displacement mixing. We focus here on their demonstration that at temperatures as low as $-120°$ C, the altered layer composition depends upon the ion current density. Their results shown in Figure 2, were obtained as follows. A 44% Au (at wt)–Cu alloy was first sputtered at $-120°$ C with 2-keV Ar ions at the indicated current density until steady state was achieved; the altered layer composition was subsequently monitored using low energy AES while sputtering at a current density of only 0.4 μA/cm^2. From Figure 2, we see that the high current density sputtering leaves the very near-surface concentration essentially equal to that of the bulk, but a subsurface, Au-depleted layer is generated which extends over the penetration depth of the ions (~ 2 nm). As discussed later, normal radiation enhanced diffusion is nonexistent at these low temperatures. Nevertheless, the altered layer which is produced indicates that Gibbsian adsorption of Au atoms to the bombarded surface is playing a prominent role in the resulting composition change. That is, the displacement mixing process is driving the alloy toward its thermodynamic end state in which the outermost atom layer is enriched in Au.

As discussed by Averback [11], recent work has made it clear that thermodynamic considerations are important in determining the atomic rearrangements produced by single cascades. For interpreting the results in Figure 2, however, it is important to realize that the technique employed by Li, Koshikawa and Gato is not sensitive to individual cascade events. It is only when cascades produced by one ion interfere
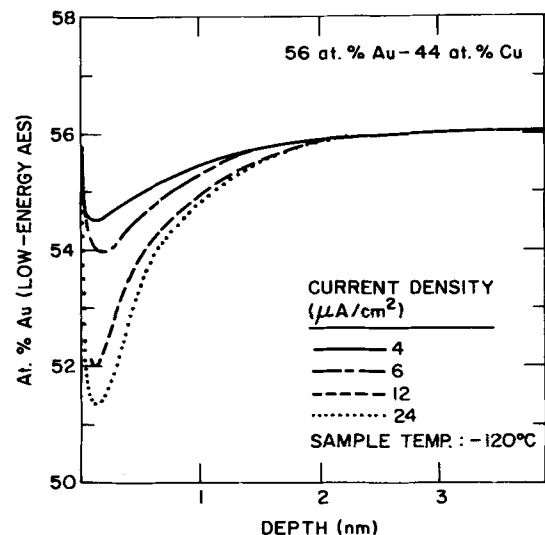

Fig. 2. Low energy AES profiles of the gold concentration in a 44% Au (at. wt.)–Cu alloy after sputtering with 2 keV Ar ions at $-120°$ C to a dose of 4×10^{17} ions/cm^2 at the indicated current densities. Profiling was done with a current density of 0.4 μA/cm^2.

dynamically with cascades produced by a second ion that an effect of ion current density can arise. The important information contained in the observed dose rate dependence is therefore the time scale over which the dynamic interference occurs. To estimate this, we convert the current density of 4 μA/cm^2 to the corresponding particle density impingement rate of 2.5 $\times$ 10^{13} ions/cm^2 s. The areal density of atoms on the specimen surface is $\sim$2 $\times$ 10^{15} atoms/cm^2. Assuming each ion affects a cylinder with a diameter of approximately 50 nm (200 interatomic distances), each atom will be involved in a cascade event on the average of

once every $\dfrac{2 \times 10^{15}}{\pi(100)^2 2.5 \times 10^{13}}$ seconds = 2.5 $\times$ 10^{-3}

s. The observable onset of a dose-rate effect should occur when the overlap is on the order of a few percent of this value. The results therefore suggest that the dynamic events within the cascade which produce Au enrichment at the surface occur over time periods extending up to $\sim$10^{-4} s after the initial knock on event.

A time scale of 10^{-4} s is considerably longer than is expected on the basis of computer simulations of cascade development using molecular dynamics, which suggest that "effective temperatures" within cascades in metals decrease to below 300 K in times on the order of 10^{-11} s. This large discrepancy between experiment and theory is currently not understood.

DEFECT MIGRATION PROCESSES: RADIATION ENHANCED DIFFUSION AND RADIATION INDUCED SEGREGATION

At temperatures where defects become mobile, mass transport occurs. Since defect concentrations well in excess of thermal equilibrium values can be generated, diffusion rates can be greatly accelerated using irradiation. If the compositional distribution in the target is already in equilibrium, this radiation enhanced diffusion (RED) will leave the distribution of alloying components unaltered. However, in targets where preferential sputtering or Gibbsian adsorption has produced an altered surface layer, RED will tend to smooth the existing gradients, and to increase the altered layer thickness.

The same defects which are responsible for RED can also produce radiation induced segregation (RIS). In general, vacancy and/or interstitial defects in alloys preferentially migrate via particular alloying elements. Because of this preferential coupling of some alloying elements to the defect fluxes, certain elements will be swept into and other elements out of local regions which experience a net influx or outflow of defects. In this manner, RIS can generate concentration gradients during irradiation of homogeneous

alloys even in the absence of preferential sputtering and Gibbsian segregation. RIS is a quite general phenomenon during irradiation, and recent reviews are available [6,21,22].

Because long-range defect migration requires that both vacancies and interstitials are mobile, temperatures well above room temperature are required in most metals before RED and RIS effects become significant. One of the earliest systematic studies of elevated target temperatures on sputter-induced surface compositional changes was an AES study by H. Shimizu et al. [23] on Cu–Ni alloys. They found a strong dependence of the measured near-surface composition on temperature during sputtering in the range of 100 to 600° C, but unfortunately were unable to measure changes during sputtering. Large effects noticed during specimen cooling to the measurement temperature complicated the interpretation of their results. Since the sputter yields of pure metals are practically independent of temperature up to almost the melting point, the apparent temperature dependence noted by Shimizu et al. was an early indication of the importance of defect migration processes in sputter-induced compositional changes at elevated temperature.

Rehn et al. [24] used AES measurements taken at temperature during sputtering of a Cu–Ni alloy to show that above 300° C, the sputtering time required to reach steady-state conditions in the near-surface region increased strongly with increasing temperature. These measurements further revealed that the degree of nickel enrichment in the subsurface layers increased steadily as the temperature was raised from 300 through 600° C. The fact that the subsurface nickel enrichment significantly exceeded that at the surface demonstrated that Gibbsian adsorption of Cu, which is known to be strong in Cu–Ni alloys, was playing a major role in the formation of the altered layer. To obtain further information about the subsurface changes, these specimens were cooled quickly immediately after the elevated temperature sputtering, and the composition was profiled at room temperature. These results are shown in Figure 3. The most striking feature is the depth to which the composition was altered during the elevated temperature sputtering. Deviations from the bulk composition are evident up to depths of $\sim$1 and 3 μm, respectively, for the specimens sputtered at 500 and 600° C. These depths are orders of magnitude greater than the penetration depth of the 5-keV Ar ions used in the experiment, which have a projected range of less than 3 nm. The large depths demonstrate that appreciable diffusion occurs at the elevated temperatures due to mobile point defects created by irradiation.

Swartzfager, Ziemecki and Kelley [25] used ISS to perform a similar elevated temperature study on low-energy ion bombarded Cu–Ni and Au–Pd alloys. An
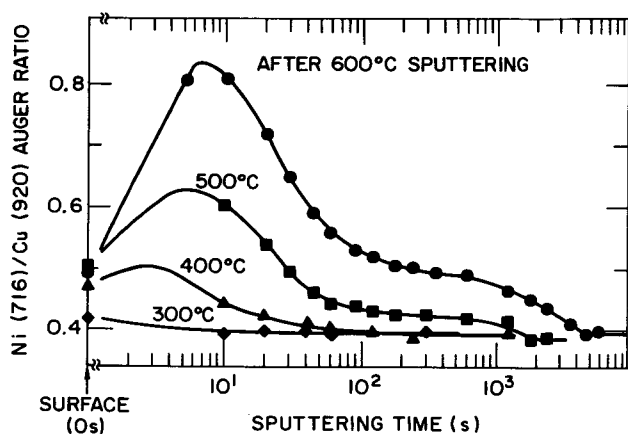
Fig. 3. AES measurements at room temperature of Ni-enriched altered layers produced in a 40% Cu (at. wt.)–Ni alloy by sputtering for two hours at the indicated elevated temperatures with 5 keV Ar ions at a current density of 195 $\mu A/cm^2$.

important first in their work was the use of a model, originally developed by Ho [26], to extract radiation enhanced diffusion coefficients, D_{RED}, from measurements of altered layer thicknesses. By assuming that the diffusion in the subsurface is enhanced uniformly, Ho has shown that at steady state, the concentration of element a in the altered layer, C_a, can be written as a function of the depth, x, from the surface ($x = 0$) in the following manner:

$$C_a(x) = A \exp\left(\frac{-x}{\delta}\right) + C_a(\infty), \qquad (4)$$

where $\delta = D_{RED}/\dot{x}$ with $\dot{x}$ being the surface recession velocity during sputtering. Some results from Swartzfager et al. [25] for Cu–Ni are shown in an Arrhenius plot in Figure 4. The surface recession velocity for these measurements was $5.2 \times 10^{-3} nm \cdot s^{-1}$. The sharply sloping solid line at the left side of the figure is an extrapolation of bulk interdiffusion data obtained at higher temperatures. As expected, the radiation enhanced diffusion coefficients exceed the normal diffusion coefficients by several orders of magnitude at low temperatures. The weak temperature dependence seen in Figure 4 below ~350° C indicates that in this regime, the defects annihilate predominantly at fixed sinks. Annihilation at fixed sinks is also in agreement with their finding that the magnitude of the radiation-enhanced diffusion coefficient was directly proportional to the ion current density. As the equilibrium vacancy concentration becomes increasingly significant at higher temperatures, D_{RED} gradually approaches the normal equilibrium values.

A very complete and systematic ISS study of near-surface compositional changes during low-energy ion
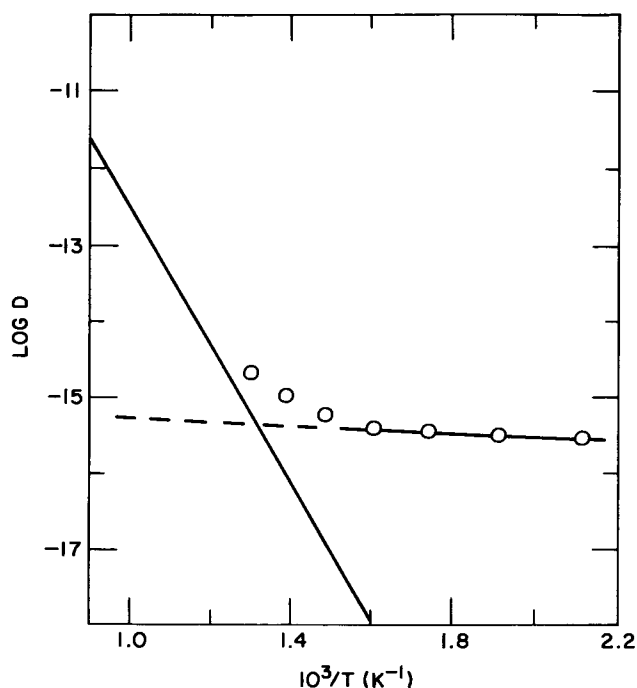

Fig. 4. Arrhenius plot of the radiation enhanced diffusion coefficients obtained by Swartzfager et al. during sputtering of a 50% Cu (at. wt.)–Ni alloy with 2 keV Ne ions at a current density of 2.5 $\mu A/cm^2$.

bombardment of Cu–Ni alloys was published by Lam et al. [27]. The measurements of subsurface compositional changes were in good agreement with the studies discussed above. However, Lam et al. noted that during sputtering above ~400° C, the steady-state concentration of the outermost atom layer was noticeably temperature dependent. Their results are shown in Figure 5, where the time evolution of the Cu/Ni ISS ratio measured during sputtering of a 40% Ni (at wt)–
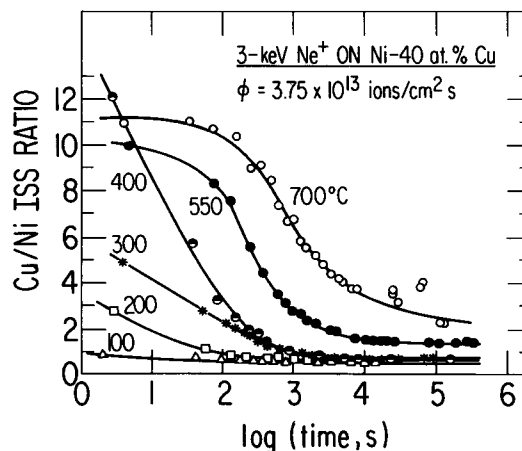

Fig. 5. Time evolution of the Cu/Ni ISS ratio measured during 3-keV Ne sputtering of a 40% Ni (at. wt.)–Cu alloy at various temperatures.

Cu alloy with 3-keV Ne ions at several different temperatures is plotted. Longer times are required to reach steady state at higher temperatures because of the increasing thicknesses of the altered layers. For temperatures above 400° C, however, the steady-state concentration of Cu also increases with increasing temperature. The temperature dependence of the steady-state surface concentration was interpreted in terms of a significant (~35%) contribution from the second atomic layer to the sputtered atom flux. The interpretation was supported by a comparison of the experimental results to compositional changes calculated using a detailed model of sputter induced compositional effects developed by Lam and Wiedersich [5].

These studies of RED during low energy ion bombardment demonstrate that large fluxes of point defects are generated during low energy bombardment which, at elevated temperatures, migrate well into the interior of the Cu–Ni specimens. Previously, it has been shown that high energy (MeV) ions, which create defect fluxes from deep (~1 μm) in the specimen toward the irradiated surface, produce a nickel-enriched surface layer at elevated temperature due to RIS [28]. That is, in Cu–Ni alloys it is known that nickel is preferentially transported in the same direction as the defect fluxes. Therefore, RIS should also result in the preferential transport of nickel into the specimen during low energy bombardment. The first observation of the RIS contribution to subsurface composi-

tional changes during low-energy bombardment was reported last year [29].

AES was used to depth-profile compositional changes produced in a 40% Cu (at wt)–Ni specimen by 5-keV Ar bombardment at elevated temperatures. Measurements of the additional nickel found at various depths after sputtering at 500° C for times of 720, 3600 and 7200 s with a current density of 180 μA/cm^2 are shown in Figure 6. Here the difference between the nickel concentration measured after the indicated sputtering time and that measured after sputtering deep into the bulk alloy is plotted on a logarithmic scale as a function of sputtering time at room temperature. All the data points given in Figure 6 are for depths (>6 nm) which are significantly greater than the ion range (≤3 nm).

The results reveal two different subsurface regions in which nickel enrichment is observed that decays apparently exponentially with depth. Region I, which results from the effects of RED as discussed above, exhibits a relatively steep decay over depths extending to approximately 100 nm. Region II manifests itself as a considerably shallower concentration gradient penetrating several μm's further into the specimen (a full profile is not included in the figure). This second region has been shown to result from RIS [29], that is the expected preferential transport of nickel into the specimen interior by the defect fluxes. The driving force for RIS arises from the gradient in the point defect
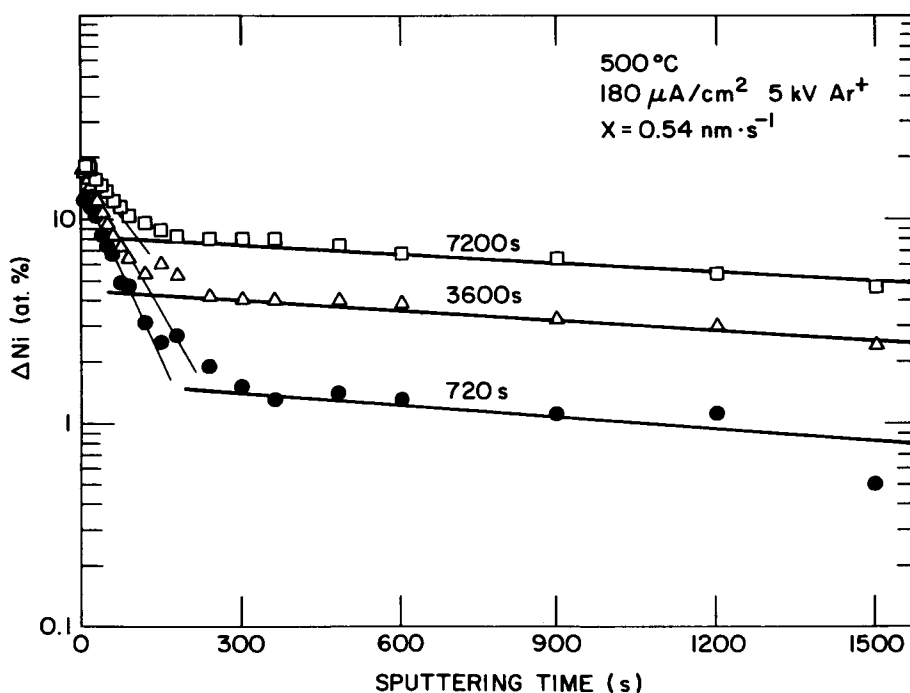

Fig. 6. Measurements of subsurface nickel enrichment produced by sputtering a 40% Cu (at. wt.)–Ni alloy with a 180 μA/cm^2 beam of 5 keV Ar ions at 500° C for the indicated times.

concentration. Hence, the decay length of the nickel enrichment in region II is proportional to the divergence of the point defect flux. The greater the decay rate of the defect concentration as a function of depth into the specimen, the smaller is the exponential decay length, δ_{II}. The magnitude of nickel enrichment at a given depth in region II increases with time as the number of defects which have annihilated at that depth increases. Note that RIS is significantly more effective than RED at producing compositional changes very deep in the specimen. This greater effectiveness may prove important in practical applications of ion-beam surface modification, where thicker altered layers usually offer distinct advantages.

Low energy ion bombardment produces steep defect concentration gradients in the very near-surface region both because of inhomogeneities in defect production as a function of depth and because of the effective defect sink provided by the external surface. Hence, RIS can be expected to be a major contributor to compositional changes in the very near-surface region during low energy ion bombardment. At present, however, there is no technique available for separating all the effects, Gibbsian adsorption, preferential sputtering, displacement mixing, RED, and RIS which contribute. A phenomenological model of sputter induced near-surface compositional changes, developed by Lam and Wiedersich [5], which incorporates all these effects is available. An attempt was made to "fit"

the experimental data shown in Figure 6 at large depths, where only RED and RIS operate, to the model, and then use the model to determine individual contributions in the near-surface region.

The time dependence of the calculated profiles at 500° C is shown in Figure 7 for an ion current density of 40 $\mu A/cm^2$; steady-state profiles at 500° C for three different ion current densities are given in Figure 8. Several qualitative features of the experimental profiles are reproduced by this set of calculations. For example, they show a relatively strong and exponential decrease in nickel enrichment over the first several tens of nanometers (region I), followed by a significantly shallower, but again exponential tail extending very deep into the specimen (region II). The time development of the calculated profiles is also qualitatively similar to that found in the experiment. The slope of region I decreases with increasing sputtering time at elevated temperature and the calculated magnitude of nickel enrichment produced by RIS in region II increases with increasing sputtering time. Furthermore, the calculated slope of Region I decreases with decreasing ion current density, as was found experimentally.

However, significant quantitative differences exist between the calculations and the experimental results. First, although the model predicts an exponential tail of nickel enrichment in region II when RIS is included, the magnitude of the calculated effect is more
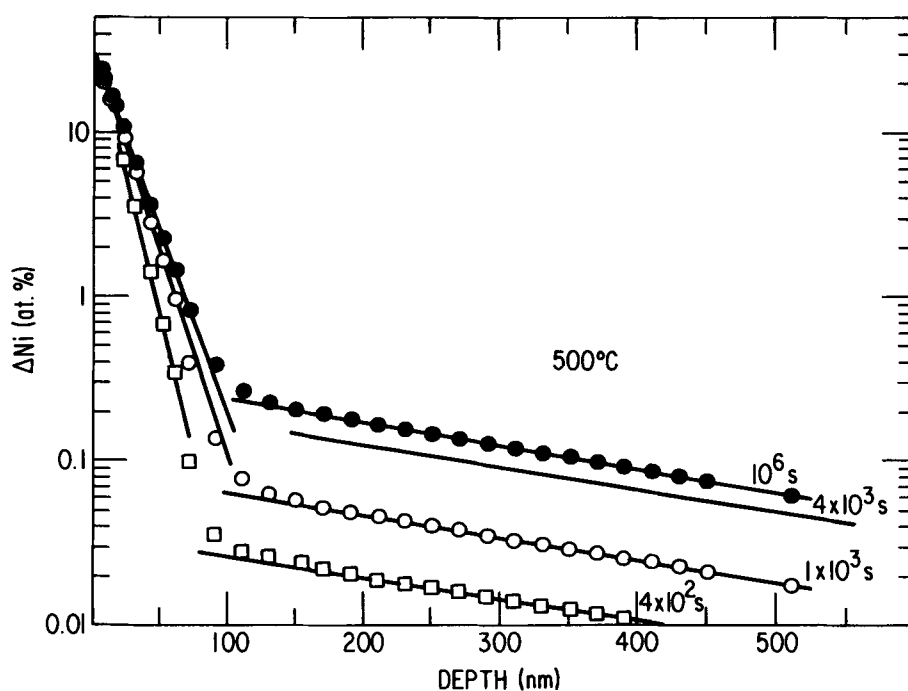

Fig. 7. Calculated time dependence of subsurface nickel enrichment in a 40% Cu (at. wt.)–Ni alloy during sputtering at 500° C with a current density of 40 $\mu A/cm^2$ of 5 keV Ar ions.
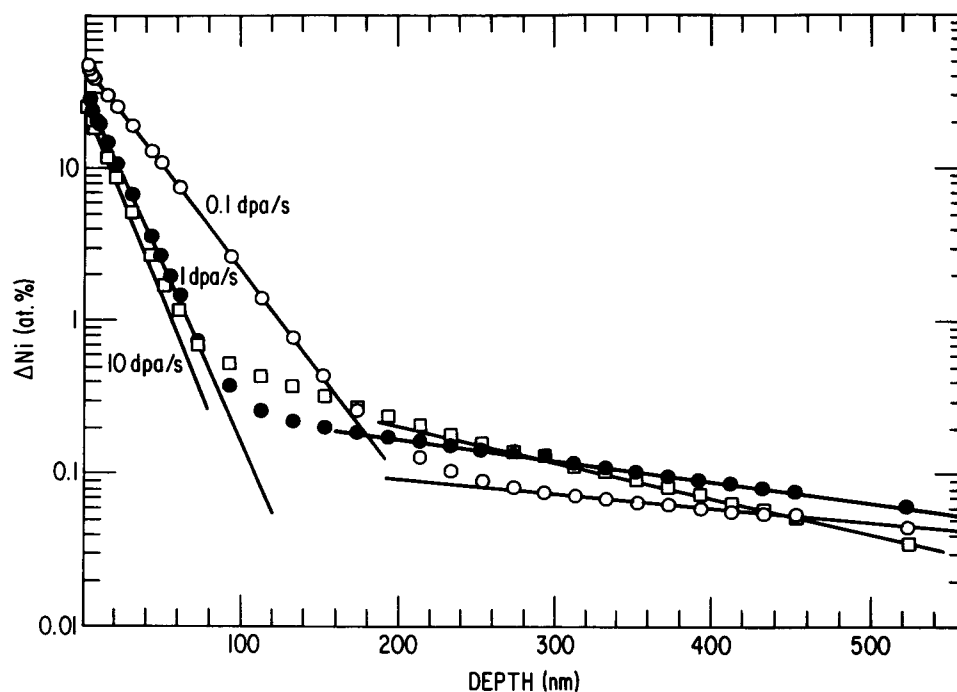
Fig. 8. Steady-state nickel enrichment profiles at 500° C calculated for ion current densities of 4, 40, and 400 μA/cm².

than an order of magnitude less than that found experimentally. Second, the calculated values of δ_I and δ_{II} are significantly smaller than the experimental values. Finally, the calculated dependence of δ_I on the sputtering rate, although predicted with the correct sign, is also significantly smaller than that observed experimentally.

The model predictions are qualitatively in agreement with the measurements. However, the large quantitative differences preclude a reliable estimate of the contribution from RIS to sputter-induced compositional changes in the very near-surface layers. In this context, however, it should be noted that the calculations do predict substantial compositional changes (several atom percent) from RIS in the very near-surface layers, despite the fact that they yield too small an effect in region II. The indication, therefore, is that RIS is an important factor in determining near-surface compositional changes during sputtering of Cu–Ni alloys at temperatures where point defects are mobile.

SUMMARY

Several processes contribute to surface compositional changes during the irradiation of alloys. These include preferential sputtering, Gibbsian adsorption, displacement mixing, radiation enhanced diffusion and, radiation induced segregation. Because of the large number of competitive processes, the temporal and spatial development of the near-surface alloy composition dur-

ing irradiation can be extremely complex. With the notable exception of preferential sputtering, however, considerable progress has been made during the past several years in identifying the relative importance of the individual processes under various irradiation conditions.

Since an appreciable fraction of sputtered atoms are emitted from subsurface atom layers, a demonstration of true preferential sputtering requires a measurement of both the composition of, and the fraction of atoms sputtered from, the individual atom layers which contribute to the flux of sputtered material. Measurements of this complexity have not yet been reported. One of the main difficulties in making such measurements is that Gibbsian segregation apparently occurs during irradiation even at very low temperatures. Hence very steep concentration gradients are generated over the same depths from which the sputtered atoms emerge.

Gibbsian adsorption during ion bombardment at low temperatures is one of several recently reported cases in which thermodynamic forces play an important role during displacement mixing. As discussed earlier, this means that the depth resolution of sputterprofiling techniques can sometimes be significantly improved by raising the specimen temperature. The dose-rate dependence of the surface composition of a Au–Cu alloy during sputtering at low temperatures reported by Li et al. suggests that dynamic interactions between individual cascades occur over time periods extending up to $\sim 10^{-4}$ s. Molecular dynamics calculations in-

dicate considerably shorter times. This discrepancy between experiment and theory is not understood.

In most alloys, defect migration assisted processes become important only at temperatures well above ambient. Radiation enhanced diffusion causes the altered layer, which is produced in the near-surface, ion-implanted region as a result of the mutual competition between all the processes, to extend to significantly greater depths at elevated temperatures. Theoretical modeling of the compositional changes beneath the implanted layer is simplified because only two processes, radiation enhanced diffusion and radiation induced segregation, operate there. Actual radiation enhanced diffusion coefficients have been extracted from measurements in this region. The compositional change due to radiation induced segregation has also been observed at large depths in the specimen. Radiation induced segregation is significantly more effective than radiation enhanced diffusion at producing compositional changes very deep in the target. This greater effectiveness may prove beneficial in practical applications of ion-beam surface modification. The prediction of current models of irradiation-induced, near-surface compositional changes are qualitatively in agreement with existing measurements, but considerably more effort is required before a quantitative, predictive capability can be achieved.

ACKNOWLEDGEMENTS

REFERENCES

1. Wynblatt et al.,
2. H.H. Anderson, *J. Vac. Sci. Technol. 16*, 1979, p. 770.
3. H. Wiedersich, in *Surface Modification and Alloying*, eds., J.M. Poate and G. Foti, Plenum Press, New York, 1983, p. 261.
4. R. Kelly, in *Symposium on Sputtering*, eds., P. Varga, G. Betz, and F.P. Viehböck Inst. of Allgem. Physik, Vienna, 1980, p. 390.
5. N.Q. Lam and H. Wiedersich, *J. Nucl. Mater. 103/104*, 1982, p. 433.
6. H. Wiedersich in *Physics of Radiation Effects in Crys-*

tals, eds. R.H. Johnson and A.N. Orlov, Elsevier Science Publishers, London, 1985, p. 225.
7. G. Betz and G.K. Wehner, in *Sputtering by Particle Bombardment II*, ed. R. Behrish (Topics in Applied Physics, Springer, Berlin, 1983, p. 11.
8. P. Sigmund, in *Sputtering by Particle Bombardment I*, ed., R. Behrish, Topics in Applied Physics, Springer, Berlin, 1983, p. 9.
9. P. Sigmund and A. Gras-Marti, *Nucl. Instr. and Meth. 182/183*, p. 35.
10. M.L. Roush, F. Davarya, O.F. Goktepe, and T.D. Andreadis, *Nucl. Instr. and Meth. 209/210*, 1983, p. 67.
11. R.S. Averback, 7th International Conference on Ion Beam Analysis, Berlin, 1985, in *J. Nucl. Mater.*; B.M. Paine and R.S. Averback, *Nucl. Instr. and Meth. B7/8*, 1985, p. 666.
12. T. Koshikawa, K. Goto, N. Saeki, R. Shimizu, and E. Suguta, *Surface Sci. 79*, 1979, p. 461.
13. T. Okutani, M. Shikata, and R. Shimizu, *Surface Sci. 99*, 1980, p. L410.
14. H.H. Andersen, B. Stenum, T. Sorensen, and H.J. Whitlow, *Nucl. Instr. and Meth. 209/210*, 1983, p. 487.
15. Y.-T. Cheng, M. Van Rossum, M-A. Nicolet, and W.L. Johnson, *Appl. Phys. Lett. 45*, 1984, p. 185.
16. W.L. Johnson, Y.-T. Cheng, M. Van Rossum, and M-A. Nicolet, *Nucl. Instr. and Meth. B7/8*, 1985, p. 657.
17. R.S. Averback, D. Peak, and L.J. Thompson, Appl. Phys. A. (in press).
18. H.H. Andersen, *Appl. Phys. 18*, 1979, p. 131.
19. M.P. Seah and M. Kühlein, *Surf. Sci. 150*, 1985, p. 273.
20. R.-S. Li, T. Koshikawa, and K. Goto, *Surf. Sci. 212*, 1982, p. L561.
21. L.E. Rehn and P.R. Okamoto, in *Phase Transformations During Irradiation*, ed. F.V. Nolfi, Jr., Applied Science Publishers, London, 1983, p. 247.
22. H. Wiedersich and N.Q. Lam, ibid., p. 1.
23. H. Shimizu, M. Ono, and K. Makayama, *J. Appl. Phys. 46*, 1975, p. 460.
24. L.E. Rehn, S. Danyluk, and H. Wiedersich, *Phys. Rev. Lett. 43*, 1979, p. 1764.
25. D.G. Swartzfager, S.B. Ziemecki, and M.J. Kelley, *J. Vac. Sci. Technol. 19*, 1981, p. 185.
26. P.S. Ho, *Surface Sci. 72*, 1978, p. 253.
27. N.Q. Lam, H.A. Hoff, H. Wiedersich, and L.E. Rehn, *Surf. Sci. 149*, 1985, p. 517.
28. W. Wagner, L.E. Rehn, H. Wiedersich, and V. Naundorf, *Phys. Rev. B28*, 1983, p. 6780.
29. L.E. Rehn, N.Q. Lam, and H. Wiedersich, *Nucl. Instr. and Meth. B7/8*, 1985, p. 764.